Published in final edited form as:
J Mol Med (Berl). 2009 January ; 87(1): 85–97. doi:10.1007/s00109-008-0409-0.

Lysophosphatidylcholine acyltransferase 1 (LPCAT1) overexpression in human colorectal cancer

Francisco Mansilla,
Molecular Diagnostic Laboratory, Center for Molecular Clinical Cancer Research, Århus University Hospital/Skejby, 8200 Aarhus, Denmark, e-mail: Francisco.mansilla@ki.au.dk

Kerry-Ann da Costa,
Department of Nutrition, University of North Carolina, Chapel Hill, NC 27599, USA

Shuli Wang,
Department of Nutrition, University of North Carolina, Chapel Hill, NC 27599, USA

Mogens Kruhøffer,
Molecular Diagnostic Laboratory, Center for Molecular Clinical Cancer Research, Århus University Hospital/Skejby, 8200 Aarhus, Denmark

Tal M. Lewin,
Department of Nutrition, University of North Carolina, Chapel Hill, NC 27599, USA

Torben F. Ørntoft,
Molecular Diagnostic Laboratory, Center for Molecular Clinical Cancer Research, Århus University Hospital/Skejby, 8200 Aarhus, Denmark

Rosalind A. Coleman, and
Department of Nutrition, University of North Carolina, Chapel Hill, NC 27599, USA

Karin Birkenkamp-Demtröder
Molecular Diagnostic Laboratory, Center for Molecular Clinical Cancer Research, Århus University Hospital/Skejby, 8200 Aarhus, Denmark

Abstract

The alteration of the choline metabolite profile is a well-established characteristic of cancer cells. In colorectal cancer (CRC), phosphatidylcholine is the most prominent phospholipid. In the present study, we report that lysophosphatidylcholine acyltransferase 1 (LPCAT1; NM_024830.3), the enzyme that converts lysophosphatidylcholine into phosphatidylcholine, was highly overexpressed in colorectal adenocarcinomas when compared to normal mucosas. Our microarray transcription profiling study showed a significant ($p<10^{-8}$) transcript overexpression in 168 colorectal adenocarcinomas when compared to ten normal mucosas. Immunohistochemical analysis of colon tumors with a polyclonal antibody to LPCAT1 confirmed the upregulation of the LPCAT1 protein. Overexpression of LPCAT1 in COS7 cells localized the protein to the endoplasmic reticulum and the mitochondria and increased LPCAT1 specific activity 38-fold. In cultured cells, overexpressed LPCAT1 enhanced the incorporation of [^{14}C]palmitate into phosphatidylcholine. COS7 cells transfected with LPCAT1 showed no growth rate alteration, in contrast to the colon cancer cell line SW480, which significantly ($p<10^{-5}$) increased its growth rate by 17%. We conclude that LPCAT1 may contribute to total choline metabolite accumulation

Correspondence to: Francisco Mansilla.

via phosphatidylcholine remodeling, thereby altering the CRC lipid profile, a characteristic of malignancy.

Keywords

Colorectal cancer; Lysophosphatidic acyltransferase; Microarrays; Lipid metabolism; Phosphatidylcholine

Introduction

Colorectal cancer (CRC) is the third most common cancer worldwide and caused almost 500,000 deaths in 2003 according to the World Cancer Report [1]. In a previous publication that analyzed pooled samples, it was discovered that an expressed sequence tag representing FLJ12443 (now known as *AYTL2*) was upregulated in CRC tissues [2]. We have now confirmed and expanded the previous observation in this new study that examined 168 colorectal adenocarcinomas and ten normal mucosa samples. We report that the *AYTL2* transcript was highly upregulated (2.5-log2-fold change) in CRC when compared to normal mucosa ($p<10^{-8}$). The encoded protein from mouse, rat, and humans for *AYTL2*, lysophosphatidylcholine acyltransferase 1 (LPCAT1; NM_024830.3), was recently characterized [3–5]. In mice and rats, LPCAT1 is predominantly expressed in lung, particularly in alveolar type II cells, where it is hypothesized to play a fundamental role in the biosynthesis of surfactant dipalmitoyl phosphatidylcholine (PtdCho). In addition, LPCAT1 shows lysophosphatidylcholine acyltransferase activity when overexpressed in COS7 or HK293 cells and has a preference for palmitate incorporation. Surprisingly, however, the human LPCAT1 was reported to be an acylglycerol-3-phosphate acyltransferase isoform (called AGPAT9), which lacked LPCAT activity when overexpressed in hamster CHO cells [5].

In higher eukaryotes, PtdCho is synthesized via two pathways, the triple methylation of phosphatidylethanol-amine (PtdEtn) and the CDP-choline pathway [6]. Remodeling allows PtdCho to exchange acyl chains by consecutive deacylation and reacylation reactions to achieve a steady-state composition of PtdCho species (Fig. 1). In the specific environment of type II pneumocytes, LPCAT1 is likely to be critical for the synthesis of dipalmitoylphosphatidylcholine by enzymatically transferring palmitoyl-CoA to the *sn*-2 position of *sn*-1 palmitoyl-lysophosphatidylcholine [4].

PtdCho is the most abundant phospholipid in both normal and malignant tissues [7,8]. In colon cancer tissues, the amount of phospholipid is highly increased [8], and increased synthesis of membrane phospholipids is required for rapid growth during tumor development [8]. In addition, changes in superficial membrane potential and phospholipid composition are associated with malignancy [9], and alterations of membrane lipid levels can also influence cell proliferation and viability [10].

In the present study, LPCAT1 was upregulated at both the transcript and protein levels in human colorectal adenocarcinomas when compared to normal mucosa. In COS7 cells, transiently overexpressed hLPCAT1 co-localized both to the endoplasmic reticulum (ER) and the mitochondria. Overexpression of LPCAT1 in COS7 cells showed no growth rate alteration, in contrast to the colon cancer cell line SW480, which showed a significant ($p<10^{-5}$) increase in growth rate. When overexpressed, hLPCAT1 catalyzed the reacylation of LysoPtdCho and had a preference for palmitoyl-CoA as its substrate. Our results suggest that, in CRC, upregulation of hLPCAT1 may contribute to increased recycling of PtdCho via

the reacylation pathway and thus contribute to an enhanced membrane synthesis and altered membrane composition.

Materials and methods

Clinical specimens

We analyzed 168 colorectal tissue samples from patients in Denmark (*n*=108), The Netherlands (*n*=56) and Finland (*n*=14), comprising 122 colon and 46 rectum cancers from Dukes stages A (1), B (149), C (13), and D (5), as described in Table 1. Ten normal mucosa biopsies from the resection edge were collected from Danish patients. Informed consent was obtained from patients, and the local scientific ethical committees approved the study.

Tissue handling, nucleic acid isolation, microsatellite analysis, gene expression analysis, and real time RT-PCR

The specimens were obtained fresh from surgery, immediately snap frozen and processed as previously described [11]. The microsatellite status of the tumors was analyzed as previously described [11]. Tumors with low-frequency MSI have similar clinical features as MSS tumors and were considered as such in this study. The readings from the quantitative scanning were analyzed by the Affymetrix Software MAS5.0. The resulting cell files for all samples were imported into ArrayAssist version 3.3 (Stratagene), and data were normalized using GC Robust Multi-array Average as implemented in ArrayAssist. *P* values in all experiments were calculated using a two-sided double *t* test with unequal variances.

Labeling of RNA, hybridization, and scanning was performed as described [11].

Semi-quantitative real-time RT-PCR was performed on 20 samples, five microsatellite unstable (MSI) and five microsatellite stable (MSS), and their corresponding matching normal mucosa. Complementary DNA (cDNA) was synthesized as described [11]. RT-PCR analysis was performed in triplicates using TaqMan® probe assay FLJ12443 ID Hs00227357_m1 (Applied Biosystems) as recommended by the manufacturers and run on a 7500 Fast Real-Time PCR system (Applied Biosystems). Results were normalized against UBC as previously described [11].

Plasmid construction

Wild-type hLPCAT1 cDNA was PCR amplified from the marathon ready colon colorectal adenocarcinoma cDNA library (Clontech) and cloned into pcDNA bidirectional (Invitrogen) using primers sense 5′-GGCGGCCATGGCTGCGGGGATG and antisense 3′-CTAATCCAGCTTCT TGC GACAGGC. Subsequently, hLPCAT1, lacking the TGA stop codon, was cloned into pcDNA3.1/V5-His (Invitrogen). hLPCAT1 was cloned into pGEX-1λT (GE Healthcare) using primers sense *Bam*HI-CGGATCGGATCCATGAGGCTGCGGGGATGC and antisense *Eco*RI ACGAGAGAATTCATCCAGCTTCTTGCGAACAGGC and standard cloning techniques. All DNA sequences were verified.

SNP analysis

Chromosomal DNA from 288 normal samples and 104 tumor samples were prepared using Puregene, Genomic DNA purification kit (Gentra Systems, Minneapolis, MN, USA). Single nucleotide polymorphism (SNP) analysis was performed using a custom TaqMan® SNP genotyping assay (BAB SNP-1397, Applied Biosystems) following the manufacturer's instructions. Messenger RNA (mRNA) isolated from eight tumor samples was converted to

cDNA using Superscript™ cDNA synthesis kit (Invitrogen), and the single PCR fragment expanding the SNP region was amplified and sequenced.

Production of monospecific antibodies

Polyclonal rabbit anti-LPCAT1 antibodies #EP389/SD25 were raised against the peptide CADFSPENSDAGRKPV (amino acids 514–529), conjugated to KLH. Antisera were affinity purified against the peptide (Eurogentec, Belgium).

Immunohistochemistry

Immunohistochemical analyses were performed on 4-μm paraffin-embedded formalin fixed (FFPE) specimens from colon adenocarcinomas and normal colon mucosa from the resection edges as previously described [12]. A multiple cancer tissue microarray (TMA) “T8235713-5-BC” (BioCat, Germany) was stained for LPCAT1 expression using unpurified rabbit anti-LPCAT1 (1:250).

Immunofluorescence microscopy

COS7 cells were cultured in RPMI 1640 medium supplemented with 10% fetal calf serum and 1% penicillin-streptomycin at 37°C and 5% CO_2 and transfected using Lipofectamine (Invitrogen) following the manufacturer’s instructions. Transfected COS7 cells were fixed and permeabilized with cold methanol (−20°C) at room temperature. Cells were stained with affinity chromatography purified rabbit anti-LPCAT1 (1:50), mouse monoclonal anti-prohibitin (1:50; Abcam), and mouse monoclonal anti-calreticulin, (1:40; Biovision). Secondary antibodies were goat anti-rabbit highly cross-adsorbed Alexa®Fluor 488 conjugated (Molecular Probes (1:2000)) in combination with goat anti-mouse Alexa®Fluor 546 conjugated (Molecular Probes (1:800)). Cells were stained with 4′,6-diamidino-2-phenylindole for nuclear visualization. Cells were mounted with Fluorescent Mounting Medium, DakoCytomation. Visualization was performed using a Zeiss Axiovert200M plus apotom fluorescence microscope with × 1,000 magnification. Images were merged using axiovision software.

Cell extraction, SDS gels, and Western blots

COS7 and SW480 cells transfected as above were harvested and lysed in lysis buffer (50 mM Tris–HCl pH 8.0, 150 mM NaCl, 1 mM dithiothreitol (DTT), 1% Triton X-100, and protease inhibitor Roche complete, ethylenediaminetetraacetic acid (EDTA) free). Twenty to 30 μg total protein samples were run in 12% sodium dodecyl sulfate (SDS) gels (Invitrogen) and transferred to nitrocellulose membranes. Membranes were blocked with 3% *w/v* non-fat powdered milk phosphate-buffered saline (PBS). The primary antibody was rabbit polyclonal unpurified anti-LPCAT1 (1:100) or rabbit anti-V5 (3 μg; Abcam) and the secondary antibody swine anti-rabbit HRP conjugated (1:5,000). The immunoreactive bands were visualized using ECL plus (Amersham Biosciences) and a UVP ChemiDoc-It, Imaging system, (UVP).

Proliferation assay

Cell proliferation assays were performed on COS7 cells and human SW480 colon cancer cells using CyQUANT® NF, Invitrogen. Briefly, 400 cells (COS7 or SW480) were plated per well. Cells were transfected as described above. After transfection, 1× dye binding solution was added at different times post-transfection, and fluorescence intensities were measured using a Biotek FLEX800-TBIDE fluorescence microplate reader at excitation 485/20 nm and detection 528/20 nm. Analyses were performed on 24 independent wells per time point and per plasmid construction.

LPCAT and AGPAT activity assays

COS7 cells in 100 mm dishes (5×10^6) were transfected with 10 μg pcDNA3.1/vector control or LPCAT1 construct using an Amaxa nucleofector, program A-24 in solution V. Twenty-four hours after transfection, cells were washed twice in PBS, resuspended in medium I (250 mM sucrose, 10 mM Tris–HCl pH 7.4, 1 mM EDTA), and homogenized with ten up and down strokes in a motor-driven Teflon-glass homogenizing vessel. Large debris and nuclei were removed by centrifugation at 600×g. Protein concentrations were determined by the bicinchonic acid method (Pierce).

The LPCAT assay was performed essentially as described previously [4]. The reaction contained 80 mM Tris, pH 7.6, 5 mM $MgCl_2$, 30–50 μM [^{14}C]palmitoyl- or [^{14}C] linoleoyl-CoA, and 50–200 μM 1-palmitoyl-lysophosphatidylcholine in a final volume of 100 μl. The assay was started by the addition of 5–10 μg post-nuclear supernatant from empty vector or LPCAT1 transfected COS7 cells, incubated at 30°C for 5 min and stopped by spotting 15 μl of the reaction mixture onto an LK6 thin layer chromatography (TLC) plate (Whatman) with authentic lipid standards (Avanti Polar Lipids). The plates were developed in $CHCl_3$/MeOH/H_2O (65:25:4) and [^{14}C] incorporated into phosphatidylcholine was determined by Bioscan analysis. Standards were visualized by exposure to iodine vapor.

AGPAT specific activity was assayed at 37°C in a 100-μl mixture containing 100 mM HEPES-NaOH pH 7.5, 200 mM NaCl, 10 mM EDTA, 8 mM NaF, 1 mg/ml bovine serum albumin (fatty acid free), 1 mM DTT, 5% (*w/v*) glycerol, 40 μM oleoyl-CoA, and 20 μM 1-[^{3}H]oleoyl-LPA (1 μCi, Perkin-Elmer NET-1100). The reaction was initiated by adding 8 μg post-nuclear supernatant to the assay mixture. Fifteen microliters of the reaction mixture was removed at 2, 4, and 6 min and spotted directly onto a Silica H plate (Analtech) together with authentic standards (Avanti). The radiolabeled phosphatidic acid (PA) product was separated from the radiolabeled lysophosphatidic acid (LPA) substrate in chloroform/pyridine/formic acid (88.5%) (50:30:7; *v/v*). Authentic lipid standards for LPA and PA were visualized by exposure to iodine vapor. Spots corresponding to PA were scraped into 500 μl methanol/water (1:1), Ecolite (ICN) was added, and radioactivity was quantified by scintillation counting.

Lipid metabolism

COS7 or SW480 cells in 60-mm dishes (1×10^6 cells) were transfected with 4 μg hLPCAT1: pcDNA3.1/V5-His or a pcDNA3.1/topo vector control. Twenty-four hours later, cells were incubated with trace (3 μM) or 100 μM [^{14}C] oleate (54.6 mCi/mmol) or [^{14}C]palmitate (57.5 mCi/mmol) (Perkin Elmer). After 3 h, cells were scraped and lipids were extracted into chloroform [13] and separated by TLC on silica gel G plates with $CHCl_3$/methanol/acetic acid/H_2O (50:37.5:3.5:2, *v/v*) together with authentic standards (Avanti, Alabaster, AL). Areas conforming to PC, PE, PI, and neutral lipids were counted on a Bioscan System 200 imaging scanner.

Choline metabolites

COS7 cells in 100-mm dishes were transfected with LPCAT1 or a pcDNA3.1/vector control (8 μg) with Lipofectamine (24 μg). Thirty hours later, the cells were scraped from each dish into 0.5-ml ice cold PBS, and 2 ml of ice cold methanol was added before choline and its metabolites were measured. Protein was measured by the bicinchoninic acid method (Pierce) using bovine serum albumin as the standard. Aqueous and organic compounds were separated, analyzed, and quantified directly using liquid chromatography/electrospray ionization-isotope dilution mass spectrometry after the addition of internal standards labeled with stable isotopes to correct for recovery [14].

Results

Microarray and RT-PCR

We have expanded the previous work on pooled CRC samples [2] using genome-wide expression profiling of a human genome U133plus2.0 microarray. We found overexpression of the transcript corresponding to probe 201818_at (*AYTL2*) in colon adenocarcinomas when compared to normal mucosa (Fig. 2a,b). Our study showed a significant overall 2.5-log2-fold change ($p<10^{-8}$), and a 0.8 log2-fold increase between the MSS and MSI subgroups ($p<10^{-7}$) (Table 2). RT-PCR analysis of 20 independent samples using a TaqMan probe against *AYTL2* confirmed the upregulation in adenocarcinomas compared to their matching normal mucosa from the resection edge (Fig. 2c). The overexpression of LPCAT1 transcript in CRC compared to normal mucosa is consistent in both analyses. A very low transcript level of human LPCAT1 in normal colon has recently been reported, supporting our results [5].

LPCAT1 protein is highly expressed in colon adenocarcinoma

Immunohistochemical analysis using anti-hLPCAT1 antibody was performed on FFPE from previously expression-profiled adenocarcinomas and specimens from their matching normal mucosa [15,16]. The matching normal mucosa showed weak LPCAT1 expression in the cytoplasm of the luminal part of the mucosa. The LPCAT1 protein was strongly upregulated in adenocarcinomas, showing an overall staining varying from moderate to very strong, even at early stages (Fig. 3). Total cell extracts from transiently transfected COS7 cells subjected to Western blot confirmed the specificity of the LPCAT1 antibody (Fig. 4i–j).

Upregulation was independent of Dukes stage, colon or rectum precedence, and only minimal (log2 ratio 0.2) although significant ($p=0.04$) between stages 2 and 3 (Table 1).

LPCAT1 is upregulated in several human cancers

Using a multiple cancer TMA, we analyzed the LPCAT1 protein expression pattern in 94 samples taken from 46 cancers from different locations and from 46 normal tissues. LPCAT1 was moderately or strongly expressed in normal human tissues (Fig. 1 and Table 1 in the Electronic supplementary material). Only normal ovary, pancreas, parotid, rectum, skin, and tongue were negative. All the tumor tissues, with the exception of those from adrenal gland, showed the same or stronger intensity than that of the normal tissues. LPCAT1 was strongly expressed in samples from normal and cancerous lung and liver.

Compared to normal colon and rectum mucosa, tumor samples showed overexpression of LPCAT1, consistent with the results obtained by immunohistochemical analysis of single samples and their matching mucosa. In summary, microarray data, RT-PCR, and immunohistochemistry all showed transcript and protein upregulation of LPCAT1 in colorectal cancer compared to normal mucosa.

SNP analysis

Amplification of the LPCAT1 cDNA coding sequence from an adenocarcinoma colorectal cDNA library identified a SNP, rs35452723, in position 1397, which causes a single amino acid mutation (M427T) in the corresponding codon sequence ATG/ACG. Because no validation status or heterozygosity was available, we performed a custom genotyping assay on more than 300 samples to determine whether a correlation exists between the identified mutation and the cancer phenotype. As shown in Table 2 in the Electronic supplementary material, we found no differences between the relative genotypic frequency of the ATG/ATG, ATG/ACG, or ACG/ACG alleles between normal individuals and colorectal cancer patients. In fact, 8% of the population tested was homozygotic for the M427T mutation

irrespective of cancer status. The M427T mutation lies beyond the glycerophosphate acyltransferase motifs [17], so this SNP probably does not significantly affect the activity or function of the protein.

Subcellular localization

Bioinformatic programs SOSUI (http://bp.nuap.nagoya-u.ac.jp/sosui/sosui_submit.html) and TMHMM (http://www.cbs.dtu.dk/services/TMHMM-2.0/) predicted the presence of a single transmembrane inside–outside segment of approximately 21 aa at the N terminus. This putative transmembrane helix suggested that the protein may bind to a membrane at its N-terminal end leaving the active site facing the cytoplasm as described for mitochondrial outer-membrane proteins such as Tom20, Tom70, and GPAT1 [18,19]. Moreover, topology prediction assessed by TargetP 1.1 (http://www.cbs.dtu.dk/services/TargetP/) suggested a potential mitochondrial localization. Although previous reports [3–5] had suggested an ER localization, we found that hLPCAT1 co-localizes with marker proteins on both the ER and the mitochondria. Immunofluorescence analysis in transiently transfected COS7 cells showed co-localization of LPCAT1 with the mitochondrial marker prohibitin in a diffused punctate pattern (Fig. 4H) and with the ER-marker calreticulin (Fig. 4d). Interestingly, in a time-based experiment, the overexpressed protein was present in the Golgi apparatus at about 12 h after transfection and was subsequently found in its final location in the mitochondria and ER (data not shown).

Proliferation assay

Green monkey kidney COS7 cells and the colon cancer cell line SW480 cells were transfected with LPCAT1. COS7 cells showed no difference in proliferation rate from 0 to 72 h. Thirty hours after transfection with LPCAT1, SW480 colon cancer cells showed an increased ($p<10^{-5}$) rate of proliferation compared to cells transfected with an empty vector (Fig. 5).

LPCAT1 activity and lipid metabolism

Previous studies have shown that the mouse LPCAT1 homolog exhibits acyltransferase activity with several acyl-CoA donors and LysoPtdCho acceptors [3–5]. Our human LPCAT1 clone also exhibits robust LPCAT activity. COS7 cells transfected with LPCAT1 had a 38-fold higher specific activity with [^{14}C]palmitoyl-CoA as acyl-donor than empty vector transfected cells (Fig. 6a). A sevenfold increase in LPCAT activity was observed when [^{14}C]linoleoyl-CoA was used as acyl-donor. In contrast to a report suggesting that LPCAT1 has 1-acylglycerol-3-phosphate acyltransferase (AGPAT) activity [5], AGPAT activity was identical in LPCAT1 transfected COS7 cells (4.56 nmol min^{-1} mg protein^{-1}) and in control cells (4.46 nmol min^{-1} mg protein^{-1}).

Compared with cells transfected with an empty vector, COS7 cells transfected with LPCAT1 showed no change in the incorporation of either trace or 100 μM [^{14}C]oleate into PtdCho (Fig. 7A (a,b)). However, with trace (~3 μM) or 100 μM [^{14}C]palmitate added to the medium, incorporation into PtdCho was enhanced 25% and 63%, respectively, in the LPCAT1 transfected cells (Fig. 7A (c,d)). Interestingly, overexpression of LPCAT1 in the presence of 100 μM palmitate reduced the amount of label incorporation into neutral lipid (predominantly triacylglycerol) (Fig. 7A (d)). No changes were observed in other lipids under any condition (dpm were 20,000–45,000; n=3 for each condition). When SW480 cells were transfected with an empty vector or with LPCAT1, we observed similar results (Fig. 7B). In these cells, the presence of LPCAT1 resulted in less [^{14}C]oleate incorporation into PtdCho (Fig. 7B (a,b)), whereas trace or 100 μM [^{14}C]palmitate incorporation into PtdCho (Fig. 7B (c,d)) was enhanced 19% or 31%, respectively. Despite the marked differences in radiolabeling with palmitate, we observed no differences in the amounts of PtdCho or

choline metabolites in LPCAT1 transfected COS7 cells as compared with the empty vector transfected cells (Table 3).

Discussion

The major findings of our study were that NM_024830.3 (previously called FLJ12433) was upregulated in human CRC compared to normal mucosa and encodes a protein with lysophosphatidylcholine acyltransferase activity rather than AGPAT activity. Overexpressed hLPCAT1 catalyzed the reacylation of LysoPtdCho, co-localized both to ER and mitochondria and significantly increased the growth rate of the colon cancer cell line SW480.

These findings suggest the importance of PtdCho metabolism in CRC. Increased abundance of the LPCAT1 protein was verified in CRC mucosa, which showed increased LPCAT1 staining compared to matching normal mucosa from the same patients. This upregulation in CRC was independent of the antibody used (polyclonal rabbit anti-hLPCAT1 serum or affinity chromatography purified). We extended the study to a tissue microarray with 46 tumors from different organ sites and their corresponding normal tissues. LPCAT1 was widely expressed in the human tissues. However, with the exception of adrenal tumors, protein expression was always at the same or a higher level in the cancer samples. The high protein expression in normal lung is consistent with previous RT-PCR analyses in mouse and with Northern blot analyses in rat and human tissues [3–5]. Expression was also very high in normal liver, perhaps related to the large amount of PtdCho synthesis required to replete losses in bile and secreted very-low density lipoprotein.

Although mouse and rat LPCAT1 were both characterized as lysophosphatidylcholine acyltransferases that prefer to use palmitate rather than oleate [3,4], the human LPCAT1 was reported to be an acylglycerol-3-phosphate acyltransferase isoform (called AGAPT9) that lacks LPCAT activity [5]. To determine the enzymatic activity of the human LPCAT1, we overexpressed hLPCAT1 in COS7 cells. LPCAT1 specific activity increased 38-fold with palmitate as the acyl-donor, but AGPAT activity did not increase, indicating that the transfected plasmid encodes an enzyme that catalyzes only LPCAT activity. Lack of LPCAT activity in the previous publication [5] may have resulted from a problem related to the location of the epitope tag, since our hLPCAT1 contains a V5-His epitope tag at the C-terminal rather than at the N-terminal.

Confirming the LPCAT activity, COS7 or SW480 cells incubated with [14C]oleate or [14C]palmitate showed enhanced incorporation of palmitate, but not oleate, into PtdCho; the COS7 cells also showed a concomitant decrease in [^{14}C]palmitate incorporation into triacylglycerol. Despite the higher reacylation of cellular LysoPtdCho in COS7 cells, the cells did not accumulate PtdCho or choline metabolites. This finding suggests that enhanced reacylation of LysoPtdCho may alter the turnover rate of PtdCho in cell membranes rather than their PtdCho. Furthermore, COS7 cells transfected with hLPCAT1 did not grow more rapidly or differ morphologically from COS7 cells transfected with the vector alone. A similar result was reported when rat liver CTP/phosphocholine cytidylyltransferaseα (CCTα) or human CCTβ were overexpressed in COS7 cells [20,21]. Despite an increased rate of PtdCho synthesis in these cells, PtdCho did not accumulate. Instead, the rate of PtdCho degradation was accelerated, and excess glycerophosphocholine (GPC) was released into the media [22]. These results suggest that general membrane phospholipid homeostasis is achieved by coordinated phospholipid synthesis and degradation to GPC via phospholipase A_2 activities. This homeostatic balance changes drastically in cancer. Both cellular phosphocholine and total choline metabolites are elevated in cancer cells and solid tumors [23]. Whereas normal cells contain high amounts of GPC and low amounts of

phosphocholine and total choline metabolites, in breast and ovarian cancers that progress to a malignant phenotype, one finds a low content of GPC and high amounts of phosphocholine and total choline metabolites [24]. This alteration is also observed in other types of cancer in which the amounts of phosphocholine and PtdCho accumulate [25].

CRC cells exhibit changes in both phospholipid composition and charge [9]. Moreover, PtdCho is the most prominent phospholipid species in both tumor and normal mucosa from colorectal tissues, and PtdCho content (μg lipid/g wet tissue) is increased in CRC [8]. The unaltered phospholipase A activity together with decreases in the activities of phospholipases C and D has suggested that attenuated PtdCho hydrolysis may explain the accumulation of PtdCho [8]. It has also been suggested that the increased synthesis of PtdCho could result from enhanced CTP/phosphocholine cytidylyltransferase activity caused by the presence of increased levels of the cytidylyltransferase protein [8], the rate-limiting step in the synthesis of PtdCho [26] (Fig. 1). Our studies suggest that LPCAT activity provides yet another mechanism for maintaining a high cellular content of PtdCho.

The importance of phospholipid metabolism in tumor growth is also suggested by the finding that phosphocholine (also known as phosphorylcholine) is present at high concentrations in human colon cancer specimens due, in part, to an increase in choline kinase activity [27]. Choline kinase protein is overexpressed in tumor-derived cell lines and in lung, prostate, and colorectal human cancers [28], and it may play a role in malignant transformation. In breast cancer, the net increase in phosphocholine can be explained by choline kinase, pancreas-enriched phospholipase C and phospholipase C β3 mRNA upregulation, together with lysophospholipase 1, phospholipase A2 Group IVA, and phospholipase D1 downregulation [29] (Fig. 1). Our CRC microarray analysis not only supports this general mechanism, but also shows some differences indicating diversity among different types of cancer (Fig. 1, Table 4).

We hypothesize that in CRC, the accumulation of PtdCho, independent of its source, is probably favored by the downregulated transcription of phospholipases A_2 together with reduced phospholipase D1, D2, and C transcription and activity (Table 4). In addition, overexpression of LPCAT1 can recycle lysophosphatidylcholine to PtdCho preferentially in the dipalmitoyl form [3]. This hypothesis is strengthened by the enhanced growth rate observed for SW480 colon cancer cells that overexpressed LPCAT1, but not in LPCAT1-transfected COS7 cells, which maintain a homeostatic phospholipid balance.

What is the effect of a high cellular PtdCho and phosphocholine content in colon cancer? Phospholipid accumulation increases the surface density of positively or negatively charged groups depending on the local pH values. An increase in the superficial membrane potential is associated with progress of malignancies [9], and an increase in membrane fluidity influences metastases because it affects cell adhesion [30]. In this context, shorter or unsaturated fatty acids of phospholipids reduce the Tm and change membrane curvature, thickness, and fluidity. Such changes in lipid profiles are specific to the cancer type [10] and may influence potential therapies because the dynamic and structural properties of lipid membranes can affect drug delivery by peptide-loaded liposomes [31].

In conclusion, we have described the upregulation of LPCAT1 in colorectal cancer adenocarcinomas compared to normal mucosa. The location of LPCAT1 in the ER and mitochondria links it to a functional role in recycling LysoPtdCho and increasing the palmitate content of PtdCho. Both PtdCho and phosphocholine are upregulated in CRC and exert an important although not fully understood role, in oncogenicity, including increased cell proliferation. We hypothesize that LPCAT1 contributes to total choline metabolite

accumulation in CRC via enhanced PtdCho recycling and to alter the specific lipid profile found in CRC.

Supplementary Material

Refer to Web version on PubMed Central for supplementary material.

Abbreviations

ER	endoplasmic reticulum
PtdCho	phosphatidylcholine
PtdEtn	phosphatidylethanolamine
CRC	colorectal cancer
MSS	microsatellite stable
MSI	microsatellite unstable

Acknowledgments

We are grateful to Pamela Celis, Susanne Bruun, Lisbeth Kjeldsen, and Jette Jensen for their excellent technical assistance as well as to Jeppe Praetorius, Institute of Anatomy, University of Aarhus, for confocal microscopy and Ludwig Wagner, Dept. of Medicine III, University of Vienna who kindly provided us with the GST-secretagogin construct. The work was supported by grants from the John and Birthe Meyer Foundation, the Novo Nordisk foundation, Toyota Fonden Denmark, the US National Institutes of Health (DK56598, DK59935, HL081554, and P30-DK56350), the Danish Research Council, the University and County of Aarhus, the Nordic Cancer Union, The Mads Clausen Foundation, and the Karen Elise Jensen foundation.

References

1. Stewart, BW.; Kleihues, P. World Cancer report. ISBN 92 832 0411 5. World Health Organization WHO Press; 2003. Ref Type: Report
2. Birkenkamp-Demtroder K, Christensen LL, Olesen SH, Frederiksen CM, Laiho P, Aaltonen LA, Laurberg S, Sorense FB, Hagemann R, ORntoft TF. Gene expression in colorectal cancer. Cancer Res. 2002; 62:4352–4363. [PubMed: 12154040]
3. Nakanishi H, Shindou H, Hishikawa D, Harayama T, Ogasawara R, Suwabe A, Taguchi R, Shimizu T. Cloning and characterization of mouse lung-type acyl-CoA:lysophosphatidylcholine acyltransferase 1 (LPCAT1). Expression in alveolar type II cells and possible involvement in surfactant production. J Biol Chem. 2006; 281:20140–20147. [PubMed: 16704971]
4. Chen X, Hyatt BA, Mucenski ML, Mason RJ, Shannon JM. Identification and characterization of a lysophosphatidylcholine acyltransferase in alveolar type II cells. Proc Natl Acad Sci U S A. 2006; 103:11724–11729. [PubMed: 16864775]
5. Agarwal AK, Sukumaran S, Bartz R, Barnes RI, Garg A. Functional characterization of human 1-acylglycerol-3-phosphate-O-acyltransferase isoform 9: cloning, tissue distribution, gene structure, and enzymatic activity. J Endocrinol. 2007; 193:445–457. [PubMed: 17535882]
6. Bishop WR, Bell RM. Assembly of phospholipids into cellular membranes: biosynthesis, transmembrane movement and intracellular translocation. Annu Rev Cell Biol. 1988; 4:579–610. [PubMed: 3058167]
7. White, DA. The phospholipids composition of mammalian tissues. In: Ansell, GB.; Hawthorne, JN.; Dawson, RMC., editors. Form and function of phospholipids. Amsterdam: Elsevier; 1973. p. 441-482.
8. Dueck DA, Chan M, Tran K, Wong JT, Jay FT, Littman C, Stimpson R, Choy PC. The modulation of choline phosphoglyceride metabolism in human colon cancer. Mol Cell Biochem. 1996; 20(162): 97–103. [PubMed: 8905631]

9. Dobrzynska I, Szachowicz-Petelska B, Sulkowski S, Figaszewski Z. Changes in electric charge and phospholipids composition in human colorectal cancer cells. Mol Cell Biochem. 2005; 276:113–119. [PubMed: 16132692]
10. Preetha A, Banerjee R, Huilgol N. Surface activity, lipid profiles and their implications in cervical cancer. J Cancer Res Ther. 2005; 1:180–186. [PubMed: 17998650]
11. Mansilla F, Birkenkamp-Demtroder K, Kruhoffer M, Sorensen FB, Andersen CL, Laiho P, Aaltonen LA, Verspaget HW, ORntoft TF. Differential expression of DHHC9 in microsatellite stable and instable human colorectal cancer subgroups. Br J Cancer. 2007; 96:1896–1903. [PubMed: 17519897]
12. Olesen SH, Christensen LL, Sorensen FB, Cabezon T, Laurberg S, ORntoft TF, Birkenkamp-Demtroder K. Human FK506 binding protein 65 is associated with colorectal cancer. Mol Cell Proteomics. 2005; 4:534–544. [PubMed: 15671042]
13. Bligh EG, Dyer WJ. A rapid method of total lipid extraction and purification. Can J Biochem Physiol. 1959; 37:911–917. [PubMed: 13671378]
14. Koc H, Mar MH, Ranasinghe A, Swenberg JA, Zeisel SH. Quantitation of choline and its metabolites in tissues and foods by liquid chromatography/electrospray ionization-isotope dilution mass spectrometry. Anal Chem. 2002; 74:4734–4740. [PubMed: 12349977]
15. Birkenkamp-Demtroder K, Olesen SH, Sorensen FB, Laurberg S, Laiho P, Aaltonen LA, ORntoft TF. Differential gene expression in colon cancer of the caecum versus the sigmoid and rectosigmoid. Gut. 2005; 54:374–384. [PubMed: 15710986]
16. Kruhoffer M, Jensen JL, Laiho P, Dyrskjot L, Salovaara R, Arango D, Birkenkamp-Demtroder K, Sorensen FB, Christensen LL, Buhl L, Mecklin JP, Jarvinen H, Thykjaer T, Wikman FP, Bech-Knudsen F, Juhola M, Nupponen NN, Laurberg S, Andersen CL, Aaltonen LA, ORntoft TF. Gene expression signatures for colorectal cancer microsatellite status and HNPCC. Br J Cancer. 2005; 20(92):240–2248.
17. Lewin TM, Wang P, Coleman RA. Analysis of amino acid motifs diagnostic for the sn-glycerol-3-phosphate acyltransferase reaction. Biochemistry. 1999; 38:5764–5771. [PubMed: 10231527]
18. Gonzalez-Baro MR, Granger DA, Coleman RA. Mitochondrial glycerol phosphate acyltransferase contains two transmembrane domains with the active site in the N-terminal domain facing the cytosol. J Biol Chem. 2001; 276:43182–43188. [PubMed: 11557771]
19. Rapaport D. Finding the right organelle. Targeting signals in mitochondrial outer-membrane proteins. EMBO Rep. 2003; 4:948–952. [PubMed: 14528265]
20. Walkey CJ, Kalmar GB, Cornell RB. Overexpression of rat liver CTP:phosphocholine cytidylyltransferase accelerates phosphatidylcholine synthesis and degradation. J Biol Chem. 1994; 269:5742–5749. [PubMed: 8119913]
21. Lykidis A, Murti KG, Jackowski S. Cloning and characterization of a second human CTP:phosphocholine cytidylyltransferase. J Biol Chem. 1998; 273:14022–14029. [PubMed: 9593753]
22. Baburina I, Jackowski S. Cellular responses to excess phospholipid. J Biol Chem. 1999; 274:9400–9408. [PubMed: 10092620]
23. Glunde K, Jie C, Bhujwalla ZM. Mechanisms of indomethacin-induced alterations in the choline hospholipid metabolism of breast cancer cells. Neoplasia. 2006; 8:758–771. [PubMed: 16984733]
24. Aboagye EO, Bhujwalla ZM. Malignant transformation alters membrane choline phospholipid metabolism of human mammary epithelial cells. Cancer Res. 1999; 59:80–84. [PubMed: 9892190]
25. Ackerstaff E, Glunde K, Bhujwalla ZM. Choline phospholipids metabolism: a target in cancer cells? J Cell Biochem. 2003; 90:525–533. [PubMed: 14523987]
26. Vance JE, Vance DE. Phospholipid biosynthesis in mammalian cells. Biochem Cell Biol. 2004; 82:113–128. [PubMed: 15052332]
27. Nakagami K, Uchida T, Ohwada S, Koibuchi Y, Suda Y, Sekine T, Morishita Y. Increased choline kinase activity and elevated phosphocholine levels in human colon cancer. Jpn J Cancer Res. 1999; 90:419–424. [PubMed: 10363580]
28. Ramirez de MA, Rodriguez-Gonzalez A, Gutierrez R, Martinez-Pineiro L, Sanchez J, Bonilla F, Rosell R, Lacal J. Overexpression of choline kinase is a frequent feature in human tumor-derived

cell lines and in lung, prostate, and colorectal human cancers. Biochem Biophys Res Commun. 2002; 296:580–583. [PubMed: 12176020]

29. Glunde K, Jie C, Bhujwalla ZM. Molecular causes of the aberrant choline phospholipid metabolism in breast cancer. Cancer Res. 2004; 64:4270–4276. [PubMed: 15205341]
30. Zeisig R, Koklic T, Wiesner B, Fichtner I, Sentjurc M. Increase in fluidity in the membrane of MT3 breast cancer cells correlates with enhanced cell adhesion in vitro and increased lung metastasis in NOD/SCID mice. Arch Biochem Biophys. 2007; 459:98–106. [PubMed: 17222386]
31. Jorgensen K, Hoyrup P, Pedersen TB, Mouritsen OG. Dynamical and structural properties of lipid membranes in relation to liposomal drug delivery systems. Cell Mol Biol Lett. 2001; 6:255–263. [PubMed: 11598644]

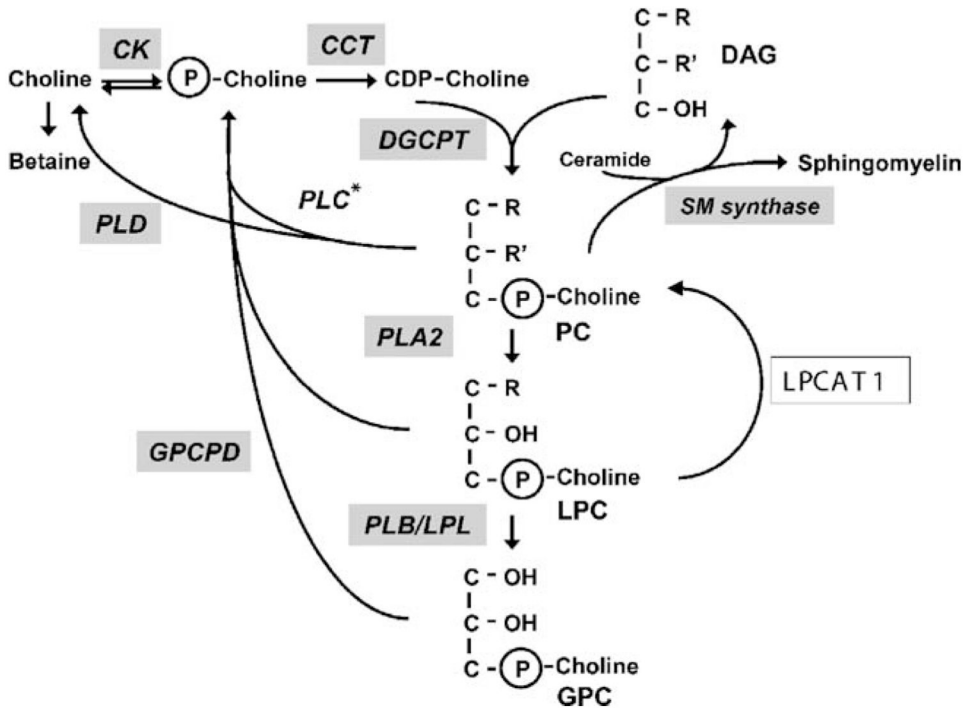

Fig. 1.

Role of hLPCAT1 in phosphatidylcholine metabolism. hLPCAT1 catalyzes the conversion of LysoPtdCho into PtdCho using palmitate preferentially as its substrate. The enzymes involved in PtdCho metabolism are highlighted in *gray squares*. *PLC** phospholipase C, the activity that hydrolyzes phsophatidylcholine to DAG and P-choline has not yet been characterized in human; *CK* choline kinase; *CCT* CTP/phosphocholine cytidylyltransferase; *PLD* phospholipase D; *DGCPT* diacylglycerol cholinephosphotransferase; *PLA2* phospholipase A_2; *GPCPD* glycerophosphocholine phosphodiesterase; *PLB/LPL* phospholipase B or lysophospholipase; *SM synthase* sphingomyelin synthase. Metabolites are *DAG* diacylglycerol, *PtdCho* phosphatidylcholine, *LysoPtdCho* lysophosphatidylcholine, *GPC* glycerophosphocholine

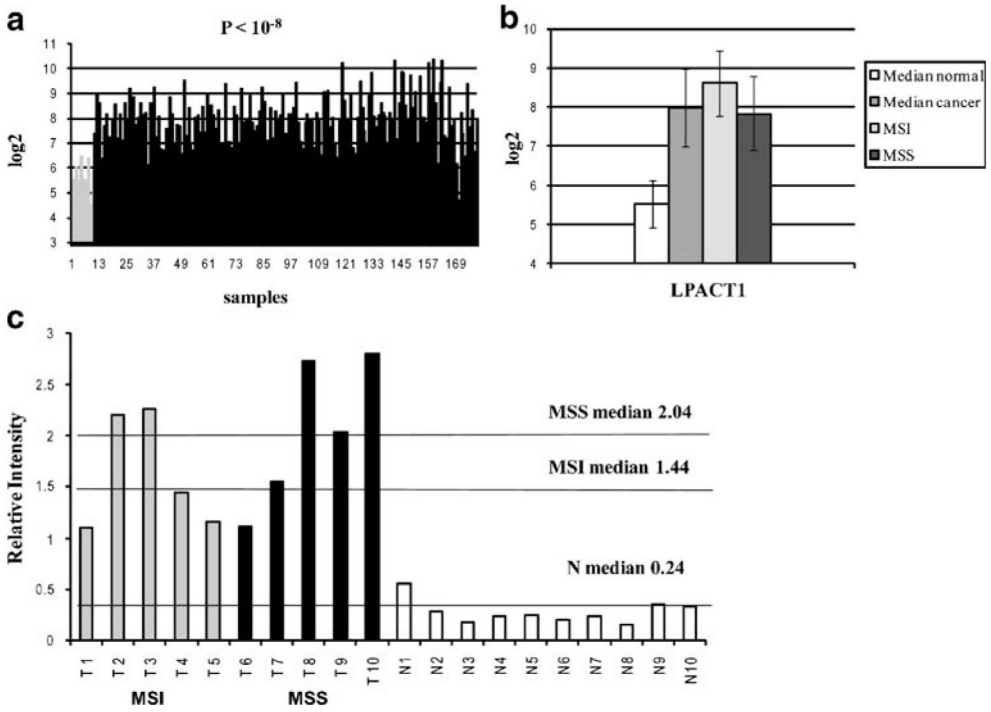

Fig. 2.

Microarray analysis of 168 samples representing molecular subgroups of colorectal cancers and real-time PCR analysis. **a** Transcript expression level of LPCAT1 on the U133plus2.0 Gene Chip. *The black bars* correspond to colorectal cancer samples, the *gray bars* to normal mucosa. Expression values are given as log2 values and all data are normalized. **b** MSS/MSI study. Median log2 values and standard deviations of normal biopsies (median normal, *n*=10), colorectal cancer patients (median cancer, *n*=168), microsatellite instable MSI (CRC patients with MSI, *n*=35), microsatellite stable MSS (CRC patients with MSS, *n*=118). **c** Real-time PCR analysis was performed in triplicates using TaqMan® probe assay FLJ12443 ID Hs00227357_m1. Each column represents a single sample. Five MSI (*gray*) and MSS (*black*) tumor samples named T1–T5, T6–T10 are represented together with their normal matching mucosa (*white*) named N1–N10. The relative intensity of LPCAT transcript has been normalized against ubiquitin

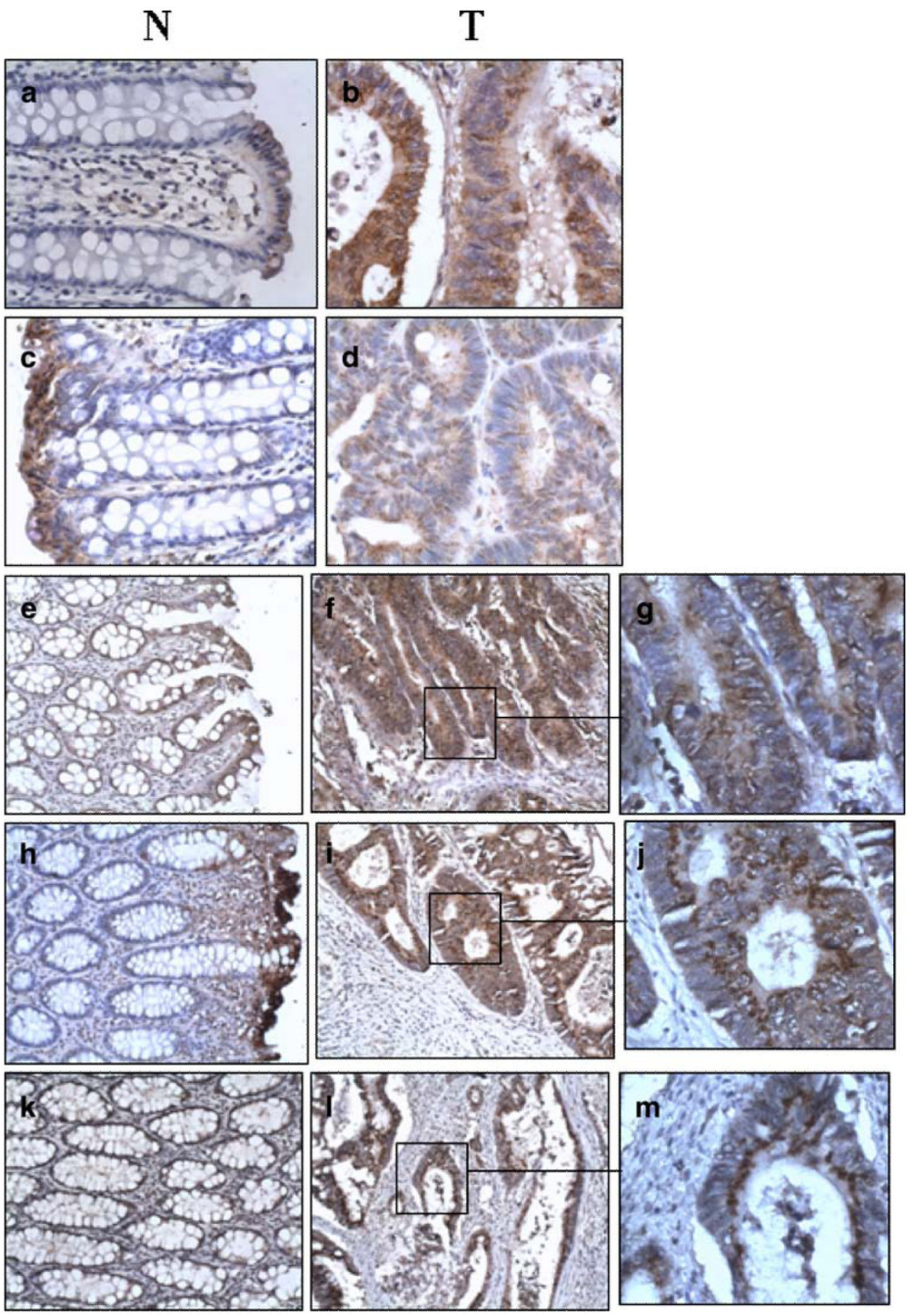

Fig. 3.

Immunohistochemical analysis of the expression of hLPCAT1 in four colon adenocarcinomas (*T*) and their respective matching normal mucosas (*N*). Magnification ×20 using unpurified rabbit anti-LPCAT1 (1:250). **a, c, e, h** Normal mucosa; **b, d, f, i** colon adenocarcinoma; **k** normal mucosa; and **l** colon adenocarcinoma from a commercial tissue microarray, ×20 magnification; **g, j, m** zoomed images from **f, i**, and **l**, ×40 magnification

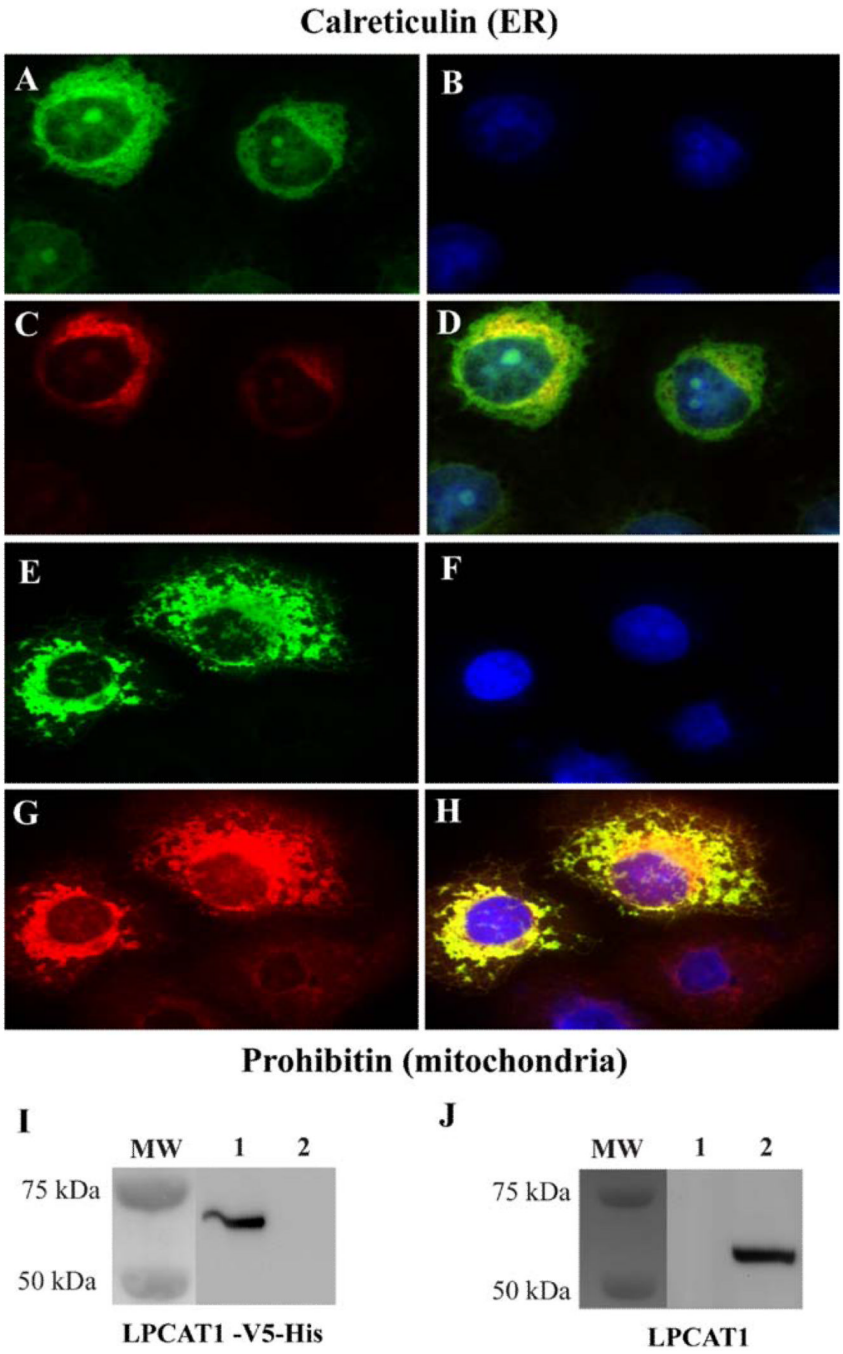

Fig. 4.

Localization of hLPCAT1 at two different sites in transiently transfected COS7 cells. **a–d** Co-localization of LPCAT1 with the ER marker calreticulin. **a** LPCAT1, **b** nucleus **c** calreticulin, **d** merged image (**a–c**). **e–h** Co-localization of LPCAT1 with the mitochondrial marker prohibitin, **e** LPCAT1, **f** nucleus, **g** prohibitin, **h** merged image. Western blot (**i–j**) COS7 cells transiently transfected with recombinant **i** hLPCAT1-V5-His or **j** hLPCAT1. Whole-cell extract detection with anti-V5 antibody (**i**) or unpurified rabbit anti-hLPCAT1 (**j**). **i** *MW* Molecular weight marker, *1* LPCAT1-V5-His, 2 mock, empty vector. **j** *MW* Molecular weight marker, *1* mock, empty vector, *2* LPCAT1

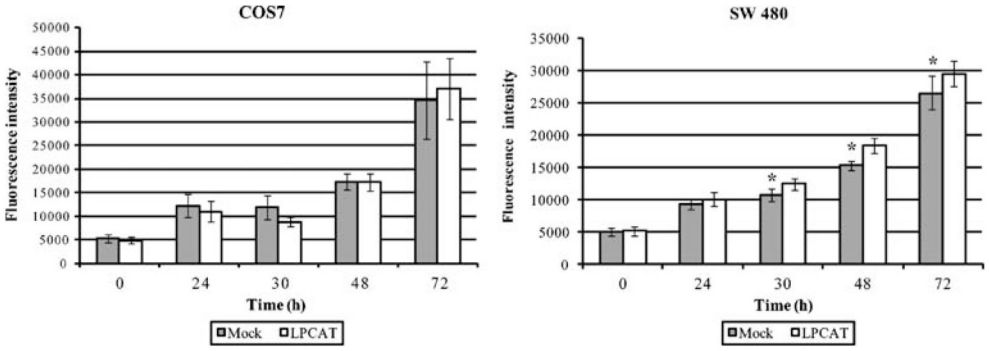

Fig. 5.

Proliferation assay Green monkey kidney COS7 cells and colorectal carcinoma SW480 cells were transiently transfected with hLPCAT1 or a mock, empty vector. Cell proliferation rate was compared at different time points. The median value of 24 independent wells is shown together with the standard deviation. After 30 h LPCAT1 transfected SW480 cells showed a significantly (*asterisk*) increased proliferation rate compared to cells transfected with an empty vector (mock). No increased proliferation rate was detected in COS7 cells transfected with hLPCAT1. **p* values are $p<10^{-5}$, $p<10^{-11}$, and $p<10^{-6}$ after 30, 48, and 72, respectively

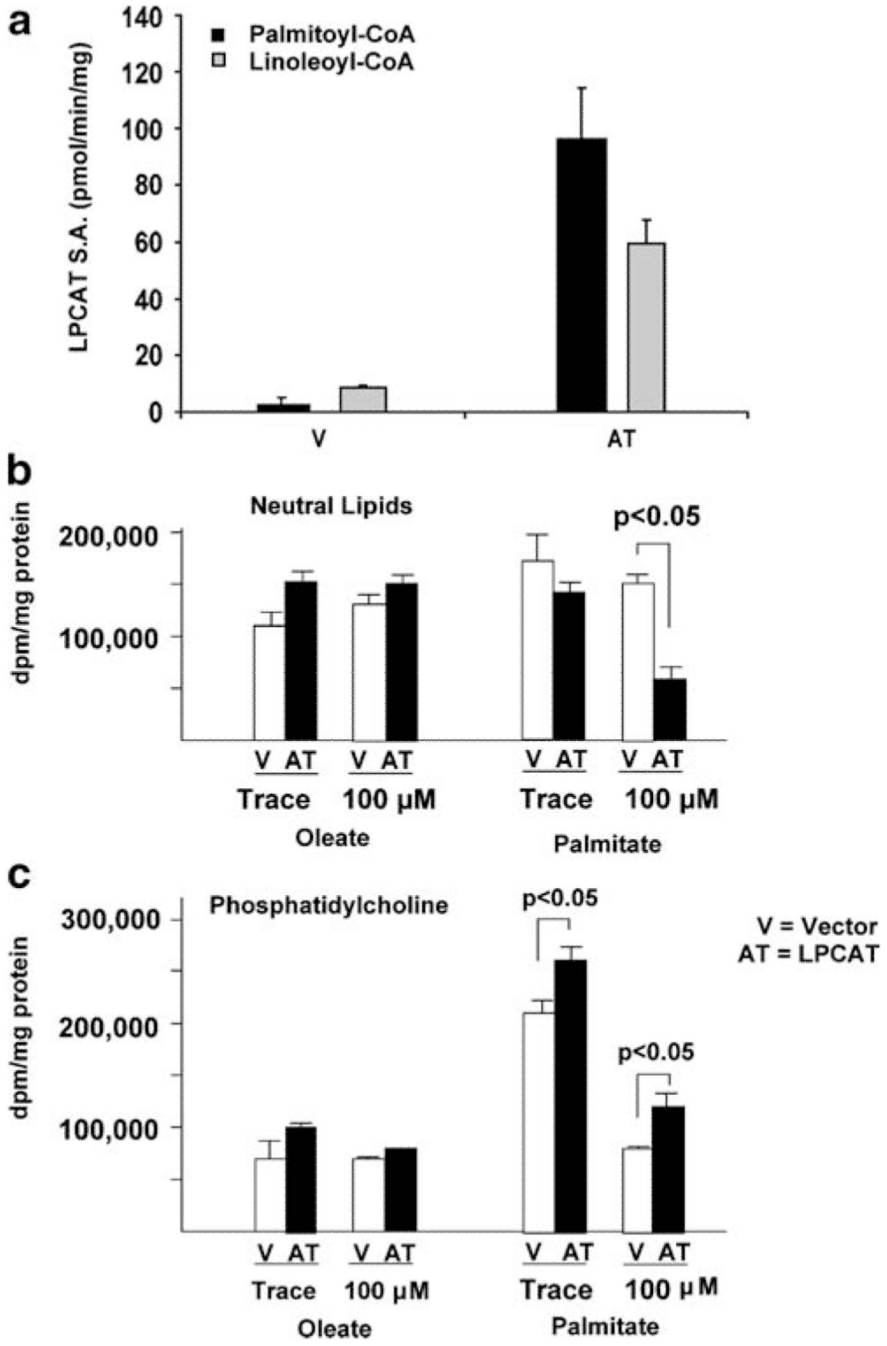

Fig. 6.

a–c Functional characterization of hLPCAT1. LPCAT1 activity was assayed as described in "Materials and methods." Post nuclear supernatant was isolated from COS7 cells transfected with empty vector (*V*) or LPCAT1-V5 (*AT*) and assayed in the presence of [^{14}C] palmitoyl-CoA or [^{14}C]linoleoyl-CoA. Data are representative of an experiment repeated three times. Fatty acid incorporation into COS7 cells transfected with LPCAT1 (*AT*) or a vector control (*V*). Twenty-four hours after transfection, cells were incubated with trace or 100 µM [^{14}C]oleate or [^{14}C]palmitate. After 60 min, cells were scraped and lipids were extracted into chloroform and separated by thin layer chromatography together with authentic

standards. [^{14}C] Fatty acid incorporation into lipids was determined by Bioscan analysis. Incorporation of [^{14}C]oleate or [^{14}C]palmitate into **b** neutral lipids or **c** PtdCho

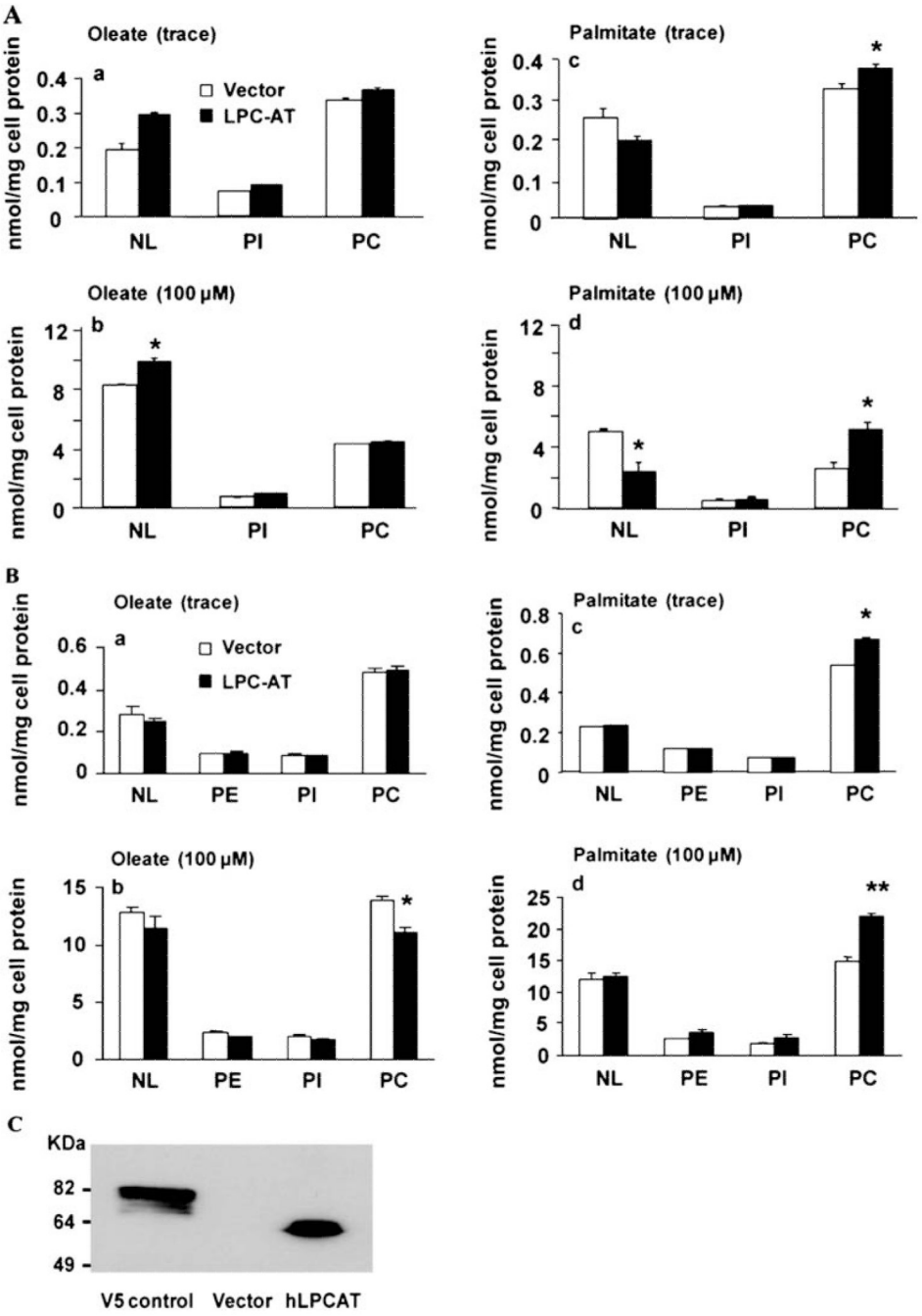

Fig. 7.

hLPCAT increases phosphatidylcholine synthesis from palmitate. Fatty acid incorporation into **a** COS7 cells or **b** SW480 cells transfected with LPCAT1 or a vector control. Twenty-four hours after transfection, cells were incubated with trace or 100 μM [^{14}C] oleate or [^{14}C]palmitate. After 3 h, cells were scraped and lipids were extracted into chloroform and separated by thin layer chromatography together with authentic standards. [^{14}C] Fatty acid incorporation into lipids was determined by Bioscan analysis. Incorporation of [^{14}C]oleate (**a, b**) or [^{14}C]palmitate (**c, d**) into neutral lipids (*NL*), phosphatidylethanolamine (*PE*), phosphatidylinositol (*PS*), or phosphatidylcholine (*PC*). *p<0.05, **p<0.001. **c** Western blot

showing SW480 cells transfected with recombinant hLPCAT1-V5-His (vector) or hLPCAT1 and detected with anti-V5 antibody

Table 1

Microarray analysis résumé table and clinical specimens

	Tumor specimens (168)	Normal specimens (10)	*p* value
Gender			
Male	91	8	
Female	77	2	
Age			
<50 years	12		
50–70 years	89	6	
>70 years	67	4	
Colon	122		0.15
Rectum	46		
Dukes' stages			
A	1		0.69
B	149		
C	13		
D	5		
Grade			
1	20		0.04
2	115		
3	30		
N.D.	3		
MSS/MSI			
MSS	118		
MSI	35		
ND	15		

Clinical specimens gender, age, Duke's stages, grade and MSS/MSI status. *p* value colon/rectum, Duke's B/A, C. D and grade 2/3

Table 2

Summary of microarray transcript profiling

	N	T	Fold change	*p* value
LPCAT1	5.5	8.0	2.5	$<10^{-8}$
MSI		8.6	3.1	MSI/MSS
MSS		7.8	2.3	$<10^{-7}$

Data are given as median log2, fold change between normal (N) and tumor (T) and p-value.

Table 3

Measurement of PC or choline metabolites in COS7 cells transiently transfected with hLPCAT1

	Betaine	Choline	GPC	PCho	PC	SM
Vector (*n*=3) nmol/mg protein	0.8±0.2	3.5±2.2	15.5±6.2	38.9±10.2	209.9±9.4	24.1±2.2
LPC-AT (*n*=3) nmol/mg protein	0.8±0.4	2.4±1.4	13.0±2.7	42.0±15.2	199.3±12.8	21.7±4.0

GPC glycerylphosphocholine, *PCho* phosphorylcholine, *PC* phosphatidylcholine, *SM* sphingomyelin

Table 4

Microarray analysis of enzymes involved in phosphatidylcholine metabolism

Protein	Normal	MSS	MSI
Choline kinase	6.4	6.5	6.3
Choline kinase	7.0	7.1	6.8
Lysophospholipase 1/phospholipase B	8.6	9.3+	8.8
Lysophospholipase 1/phospholipase B	10.8	11.1+	11.1+
Phospholipase A2 Group IVA	6.6	4.3−	6.3−
Pancreas-enriched phospholipase C	9.3	6.3−	6.7−
Pancreas-enriched phospholipase C	9.0	5.9−	6.5−
Phospholipase C β3	6.5	9.1+	9.3+
Phospholipase D1	7.0	5.2−	5.3−
Phospholipase D1	5.3	3.5−	3.6−
Phospholipase D2	6.0	5.7−	6.0
CTP phosphocholine cytidylyltransferase	ud	ud	ud
Diacylglycerol phosphotransferase	10.7	10.2−	9.9−
Phospholipase A2 group X	10.0	6.7−	7.0−
Phospholipase A2 groupXIIA	7.7	7.3−	7.6
Phospholipase A2 group XIIA	6.4	6.5	6.8+
Phospholipase A2 group XIIB	ud	ud	ud
Phospholipase A2 group IB	ud	ud	ud
Phospholipase A2 group IIA	10.1	9.0+	10.9+
Phospholipase A2 group IID	ud	ud	ud
Phospholipase A2 group IIE	ud	ud	ud
Phospholipase A2 group IIF	ud	ud	ud
Phospholipase A2 group III	ud	ud	ud
Phospholipase A2 group V	ud	ud	ud
Phospholipase A2 group VI	ud	ud	ud

Enzymes from choline kinase to phospholipase D2 correspond to those reported to be differentially expressed in breast cancer [29]. Data are given as median log2-fold change between normal (N) and tumor (*MSS* microsatellite stable or *MSI* microsatellite unstable) and with $p<0.05$. *ud* under detection, reflects log2 values<5.0 considered as background